

An Adaptive Finite Element Method for the Wave Scattering with Transparent Boundary Condition

Xue Jiang · Peijun Li · Junliang Lv ·
Weiyang Zheng

Received: date / Accepted: date

Abstract Consider the acoustic wave scattering by an impenetrable obstacle in two dimensions. The model is formulated as a boundary value problem for the Helmholtz equation with a transparent boundary condition. Based on a duality argument technique, an a posteriori error estimate is derived for the finite element method with the truncated Dirichlet-to-Neumann boundary operator. The a posteriori error estimate consists of the finite element approximation error and the truncation error of boundary operator which decays exponentially with respect to the truncation parameter. A new adaptive finite element algorithm is proposed for solving the acoustic obstacle scattering problem, where the truncation parameter is determined through the truncation error and the mesh elements for local refinements are marked through the finite element discretization error. Numerical experiments are presented to illustrate the competitive behavior of the proposed adaptive method.

Keywords Acoustic scattering problem · Adaptive finite element method · Transparent boundary condition · A posteriori error estimate

Mathematics Subject Classification (2000) 65M30 · 78A45 · 35Q60

X. Jiang
School of Science, Beijing University of Posts and Telecommunications, Beijing 100876, China.
E-mail: jxue@lsec.cc.ac.cn

P. Li
Department of Mathematics, Purdue University, West Lafayette, Indiana 47907, USA.
E-mail: lipeijun@math.purdue.edu

J. Lv
School of Mathematics, Jilin University, Changchun 130012, China.
E-mail: lvjl@jlu.edu.cn

W. Zheng
NCMIS, LSEC, ICMSEC, Academy of Mathematics and System Sciences, Chinese Academy of Sciences, Beijing, 100190, China.
E-mail: zwy@lsec.cc.ac.cn

1 Introduction

The obstacle scattering problem is referred to as wave scattering by bounded impenetrable obstacles. It usually leads to an exterior boundary value problem imposed in an open domain. Scattering theory in structures of bounded obstacles has played a fundamental role in diverse scientific areas of applications such as radar and sonar, non-destructive testing, and geophysical exploration [12]. Due to its significant industrial, medical, and military applications, the obstacle scattering problem has received considerable attention in both the engineering and mathematical communities. It has been studied extensively in the past several decades. A large amount of information is available regarding its solutions. A variety of numerical methods are proposed to solve the scattering problem such as the finite element methods [20, 21] and the boundary integral equation methods [11].

Since the problem is imposed in an open domain, the unbounded physical domain needs to be truncated into a bounded computational domain in order to apply the finite element method. Therefore, an appropriate boundary condition is needed on the boundary of the truncated domain so that no artificial wave reflection occurs. Such boundary conditions are called transparent boundary conditions or non-reflecting boundary conditions. They are still the subject matter of much ongoing research [2, 13, 15–17]. The perfectly matched layer (PML) technique is one of the effective approaches to truncate unbounded domains into bounded ones [7]. Various constructions of PML absorbing layers have been proposed and studied for wave propagation problems [10, 23, 24]. Under the assumption that the exterior solution is composed of outgoing waves only, the basic idea of the PML technique is to surround the physical domain by a layer of finite thickness with specially designed model medium that would either slow down or attenuate all the waves that propagate from the computational domain. Combined with the PML technique, effective adaptive finite element methods were proposed to solve the diffraction grating problems [4, 5, 8], where the wave is scattered by periodic structures. Due to their superior numerical performance, the methods were quickly extended to solve the obstacle scattering problem for both the two-dimensional Helmholtz equation and the three-dimensional Maxwell equations [6, 9].

Recently, an alternative adaptive finite element method was proposed for solving the same acoustic obstacle scattering problem [19], where the transparent boundary condition was used to truncate the domain. In this approach, no extra artificial domain needs to be imposed to surround the physical domain, which makes it different from the PML technique. The transparent boundary condition is based on a nonlocal Dirichlet-to-Neumann (DtN) operator, which is defined by an infinite Fourier series. Since the transparent boundary condition is exact, the artificial boundary can be put as close as possible to surround the obstacle, which can reduce the size of the computational domain and the scale of the resulting linear system of algebraic equations. Numerically, the infinite series needs to be truncated into a sum of finite sequence by choosing some positive integer N . In [19], we derived an a posteriori error estimate, which accounted for the finite element discretization error but did not incorporate the truncation error of the DtN operator. Therefore, it was ad hoc to pick an appropriate truncation number N and lacked of a rigorous analysis for the choice of this parameter.

The aim of this paper is to give a complete a posteriori error estimate and present an effective adaptive finite element algorithm. The new a posteriori error

estimate not only takes into account of the finite element discretization error but also includes the truncation error of the boundary operator. It was shown in [18] that the convergence could be arbitrarily slow for the truncated DtN mapping to the original DtN mapping in its operator norm. The a posteriori error analysis of the PML method cannot be applied to our DtN case since the DtN mapping of the truncated PML problem converges exponentially fast to the original DtN mapping. To overcome this difficulty, we adopt a duality argument and obtain an a posteriori error estimate between the solution of the scattering problem and the finite element solution. The estimate is used to design the adaptive finite element algorithm to choose elements for refinements and to determine the truncation parameter N . We show that the truncation error decays exponentially with respect to N . Therefore, the choice of the truncation parameter N is not sensitive to the given tolerance. The numerical experiments demonstrate a comparable behavior to the adaptive PML method presented in [9]. They show much more competitive efficiency by adaptively refining the mesh as compared with uniformly refining the mesh. Thus, this work provides a viable alternative to the adaptive finite element method with the PML technique for solving the acoustic scattering problem. The algorithm is expected to be applicable for solving many other wave propagation problems in open domains and even more general model problems where transparent boundary conditions are available but the PML may not be applied. We refer to [25] for a closely related adaptive finite element method with transparent boundary condition for solving the diffraction grating problem.

The outline of this paper is as follows. In section 2, we introduce the model problem of the acoustic wave scattering by an obstacle and its weak formulation by using the transparent boundary condition. The finite element discretization with truncated DtN operator is presented in section 3. Section 4 is devoted to the a posteriori error estimate by using a duality argument. In section 5, we discuss the numerical implementation of our adaptive algorithm and present some numerical experiments to demonstrate the competitive behavior of the proposed method. The paper is concluded with some general remarks and directions for future research in section 6.

2 Model problem

Consider the acoustic scattering by a sound-hard bounded obstacle D with Lipschitz continuous boundary ∂D , as seen in Figure 1. Let $B_R = \{x \in \mathbb{R}^2 : |x| < R\}$ and $B_{R'} = \{x \in \mathbb{R}^2 : |x| < R'\}$ be the balls with radii R and R' , respectively, where $R > R' > 0$. Denote by ∂B_R and $\partial B_{R'}$ the boundaries of B_R and $B_{R'}$, respectively. Let R' be large enough such that $\bar{D} \subset B_{R'} \subset B_R$. Denote by $\Omega = B_R \setminus \bar{D}$ the bounded domain, in which our boundary value problem will be formulated.

The acoustic wave propagation can be modeled by the two-dimensional Helmholtz equation

$$\Delta u + \kappa^2 u = 0 \quad \text{in } \mathbb{R}^2 \setminus \bar{D}, \quad (1)$$

where $\kappa > 0$ is a positive constant and is known as the wavenumber. Since the obstacle is sound-hard, the scattered wave field u satisfies the inhomogeneous Neumann boundary condition

$$\partial_\nu u = -g \quad \text{on } \partial D, \quad (2)$$

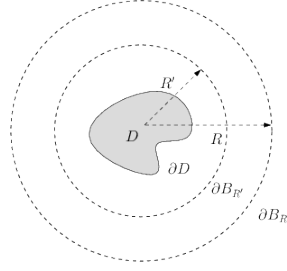


Fig. 1 Geometry of the obstacle scattering problem.

where ν is the unit outward normal vector on ∂D . In this work, we use the sound-hard boundary condition as an example to present the results. Our method can be applied to solve other type of obstacles with either the sound-soft or the impedance boundary condition. In addition, the wave field u is required to satisfy the Sommerfeld radiation condition

$$\lim_{r \rightarrow \infty} r^{1/2} (\partial_r u - i\kappa u) = 0, \quad r = |x|. \quad (3)$$

Denote by $L^2(\Omega)$ the usual Hilbert space of square integrable functions. The space is equipped with the following inner product and norm

$$(u, v) = \int_{\Omega} u(x) \bar{v}(x) dx \quad \text{and} \quad \|u\|_{L^2(\Omega)} = (u, u)^{1/2},$$

where \bar{v} denotes the complex conjugate of v . Let $H^1(\Omega)$ be the standard Sobolev space equipped with the norm

$$\|u\|_{H^1(\Omega)} = \left(\|u\|_{L^2(\Omega)}^2 + \|\nabla u\|_{L^2(\Omega)}^2 \right)^{1/2}. \quad (4)$$

For any function $u \in L^2(\partial B_R)$, it admits the Fourier series expansion

$$u(R, \theta) = \sum_{n \in \mathbb{Z}} \hat{u}_n(R) e^{in\theta}, \quad \hat{u}_n(R) = \frac{1}{2\pi} \int_0^{2\pi} u(R, \theta) e^{-in\theta} d\theta.$$

We define an equivalent $L^2(\partial B_R)$ norm of u by using the Fourier coefficients:

$$\|u\|_{L^2(\partial B_R)} = \left(2\pi \sum_{n \in \mathbb{Z}} |\hat{u}_n(R)|^2 \right)^{1/2}.$$

The trace space $H^s(\partial B_R)$ is defined by

$$H^s(\partial B_R) = \{u \in L^2(\partial B_R) : \|u\|_{H^s(\partial B_R)} < \infty\},$$

where the $H^s(\partial B_R)$ norm is given by

$$\|u\|_{H^s(\partial B_R)} = \left(2\pi \sum_{n \in \mathbb{Z}} (1 + n^2)^s |\hat{u}_n(R)|^2 \right)^{1/2}. \quad (5)$$

It is clear to note that the dual space of $H^s(\partial B_R)$ is $H^{-s}(\partial B_R)$ with respect to the scalar product in $L^2(\partial B_R)$ defined by

$$\langle u, v \rangle_{\partial B_R} = \int_{\partial B_R} u \bar{v} ds.$$

In the exterior domain $\mathbb{R}^2 \setminus \bar{B}_R$, the solution of the Helmholtz equation (1) can be written as a Fourier series in the polar coordinates:

$$u(r, \theta) = \sum_{n \in \mathbb{Z}} \frac{H_n^{(1)}(\kappa r)}{H_n^{(1)}(\kappa R)} \hat{u}_n e^{in\theta}, \quad \hat{u}_n = \frac{1}{2\pi} \int_0^{2\pi} u(R, \theta) e^{-in\theta} d\theta, \quad r > R, \quad (6)$$

where $H_n^{(1)}(\cdot)$ is the Hankel function of the first kind with order n .

Given $u \in H^{1/2}(\partial B_R)$, we introduce the DtN operator $\mathcal{T}: H^{1/2}(\partial B_R) \rightarrow H^{-1/2}(\partial B_R)$:

$$(\mathcal{T}u)(R, \theta) = \frac{1}{R} \sum_{n \in \mathbb{Z}} h_n(\kappa R) \hat{u}_n e^{in\theta}, \quad (7)$$

where

$$h_n(z) = z \frac{H_n^{(1)'}(z)}{H_n^{(1)}(z)}.$$

It follows from (6) and (7) that we have the transparent boundary condition

$$\partial_r u = \mathcal{T}u \quad \text{on } \partial B_R. \quad (8)$$

Multiplying (1) by the complex conjugate of a test function $v \in H^1(\Omega)$, integrating over Ω , and using Green's formula and the boundary conditions (2) and (8), we arrive at an equivalent variational formulation for the scattering problem (1)–(3): Find $u \in H^1(\Omega)$ such that

$$a(u, v) = \langle g, v \rangle_{\partial D} \quad \text{for all } v \in H^1(\Omega), \quad (9)$$

where the sesquilinear form $a: H^1(\Omega) \times H^1(\Omega) \rightarrow \mathbb{C}$ is defined by

$$a(u, v) = (\nabla u, \nabla v) - \kappa^2(u, v) - \langle \mathcal{T}u, v \rangle_{\partial B_R} \quad (10)$$

and the linear functional

$$\langle g, v \rangle_{\partial D} = \int_{\partial D} g \bar{v} ds.$$

Following [18, 19], we may show that the variational problem (9) has a unique weak solution $u \in H^1(\Omega)$ for any wavenumber κ and the solution satisfies the estimate

$$\|u\|_{H^1(\Omega)} \leq C \|g\|_{H^{-1/2}(\partial D)}, \quad (11)$$

where C is a positive constant depending on κ and R . Since $H^{-1/2}(\partial D)$ is not computable in the a posteriori error estimate, we rewrite the estimate (11) as

$$\|u\|_{H^1(\Omega)} \leq C \|g\|_{L^2(\partial D)}. \quad (12)$$

The general theory in Babuska and Aziz [1] implies that there exists a constant $\gamma > 0$ depending on κ and R such that it holds the following inf-sup condition:

$$\sup_{0 \neq v \in H^1(\Omega)} \frac{|a(u, v)|}{\|v\|_{H^1(\Omega)}} \geq \gamma \|u\|_{H^1(\Omega)} \quad \text{for all } u \in H^1(\Omega).$$

We collect some results from [26] on the Bessel functions before proceeding to the discrete approximation. Let $J_n(t)$ and $Y_n(t)$ be the Bessel functions with order n of the first and second kind, respectively. For any positive integer n , we have

$$J_{-n}(t) = (-1)^n J_n(t), \quad Y_{-n}(t) = (-1)^n Y_n(t).$$

The Hankel functions of the first and second kind with order n are

$$H_n^{(j)}(t) = J_n(t) \pm iY_n(t), \quad j = 1, 2.$$

For fixed $t > 0$, we have the asymptotic expressions

$$J_n(t) \sim \frac{1}{\sqrt{2\pi n}} \left(\frac{et}{2n}\right)^n, \quad Y_n(t) \sim -\sqrt{\frac{2}{\pi n}} \left(\frac{et}{2n}\right)^{-n}, \quad n \rightarrow \infty, \quad (13)$$

which gives that

$$H_n^{(j)}(t) \sim i(-1)^j \sqrt{\frac{2}{\pi n}} \left(\frac{et}{2n}\right)^{-n}, \quad n \rightarrow \infty. \quad (14)$$

These asymptotic expressions will be used in subsequent analysis.

3 Finite element approximation

Let \mathcal{M}_h be a regular triangulation of Ω , where h denotes the maximum diameter of all the elements in \mathcal{M}_h . To avoid being distracted from the main focus of the a posteriori error estimate, we assume for simplicity that ∂D and ∂B_R are polygonal to keep from using the isoparametric finite element space and deriving the approximation error of the boundaries Γ and ∂B_R . Thus any edge $e \in \mathcal{M}_h$ is a subset of $\partial\Omega$ if it has two boundary vertices.

Let $V_h \subset H^1(\Omega)$ be a conforming finite element space, i.e.,

$$V_h := \{v_h \in C(\bar{\Omega}) : v_h|_K \in P_m(K) \text{ for all } K \in \mathcal{M}_h\},$$

where m is a positive integer and $P_m(K)$ denotes the set of all polynomials of degree no more than m . The finite element approximation to the problem (9) reads as follows: Find $u_h \in V_h$ such that

$$a(u_h, v_h) = \langle g, v_h \rangle_{\partial D} \quad \text{for all } v_h \in V_h. \quad (15)$$

In the above formulation, the DtN operator \mathcal{T} defined in (7) is given by an infinite series. Practically, it is necessary to truncate the nonlocal operator by taking finitely many terms of the expansions so as to attain a feasible algorithm. Given a sufficiently large N , we define a truncated DtN operator

$$(\mathcal{T}_N u)(R, \theta) = \frac{1}{R} \sum_{|n| \leq N} h_n(\kappa R) \hat{u}_n e^{in\theta}. \quad (16)$$

Using the truncated DtN operator, we have the truncated finite element approximation to the problem (9): Find $u_h^N \in V_h$ such that

$$a_N(u_h^N, v_h) = \langle g, v_h \rangle_{\partial D} \quad \text{for all } v_h \in V_h, \quad (17)$$

where the sesquilinear form $a_N : V_h \times V_h \rightarrow \mathbb{C}$ is defined as follows:

$$a_N(u, v) = (\nabla u, \nabla v) - \kappa^2(u, v) - \langle \mathcal{T}_N u, v \rangle_{\partial B_R}. \quad (18)$$

For sufficiently large N and sufficiently small h , the discrete inf-sup condition of the sesquilinear form a_N may be established by a general argument of Schatz [22]. It follows from the general theory in [1] that the truncated variational problem (17) admits a unique solution. We also refer to [18] for the well-posedness and error analysis of the problem (18). In this work, our focus is the a posteriori error estimate and the associated adaptive algorithm. Thus we assume that the discrete problem (18) has a unique solution $u_h^N \in V_h$.

4 The a posteriori error analysis

For any $T \in \mathcal{M}_h$, denote by h_T its diameter. Let \mathcal{B}_h denote the set of all the edges of T . For any $e \in \mathcal{B}_h$, denote by h_e its length. For any interior edge e which is the common side of T_1 and $T_2 \in \mathcal{M}_h$, we define the jump residual across e as

$$J_e = -(\nabla u_h^N|_{T_1} \cdot \nu_1 + \nabla u_h^N|_{T_2} \cdot \nu_2),$$

where ν_j is the unit outward normal vector on the boundary of T_j , $j = 1, 2$. For any boundary edge $e \subset \partial B_R$, we define the jump residual

$$J_e = 2(\mathcal{T}_N u_h^N - \nabla u_h^N \cdot \nu),$$

where ν is the unit outward normal on ∂B_R . For any boundary edge $e \subset \Gamma$, we define the jump residual

$$J_e = 2(\nabla u_h^N \cdot \nu + g).$$

Here ν is the unit outward normal on ∂D pointing toward Ω . For any $T \in \mathcal{M}_h$, denote by η_T the local error estimator, which is defined by

$$\eta_T = h_T \|\mathcal{R} u_h^N\|_{L^2(T)} + \left(\frac{1}{2} \sum_{e \in \partial T} h_e \|J_e\|_{L^2(e)}^2 \right)^{1/2}, \quad (19)$$

where the residual operator $\mathcal{R} = \Delta + \kappa^2$.

For brevity, we adopt the notation $a \lesssim b$ to represent $a \leq Cb$, where the positive constant C may depend on κ, R, R' , but does not depend on the truncation of the DtN operator N or the mesh size of the triangulation h .

We now state the main result, which plays an important role for the numerical experiments.

Theorem 1 *Let u and u_h^N be the solutions of (9) and (17), respectively. There exists a positive integer N_0 independent of h such that we have the following a posteriori error estimate for $N > N_0$:*

$$\|u - u_h^N\|_{H^1(\Omega)} \lesssim \left(\sum_{T \in \mathcal{M}_h} \eta_T^2 \right)^{1/2} + \left(\frac{R'}{R} \right)^N \|g\|_{L^2(\partial D)}.$$

We remark that the first term on the right-hand side of the above estimate comes from the finite element discretization error, while the second term accounts for the truncation error of the DtN boundary operator. It is clear to note that the error arising from the second term decays exponentially with respect to N since $R' < R$.

In the rest of this section, we shall prove the a posteriori error estimator in Theorem 1 by adopting a duality argument, which is used in [3, 22] for a priori error estimates of indefinite problems and in [25] for a posteriori error estimate for the diffractive grating problem.

Denote the error $\xi := u - u_h^N$. Introduce a dual problem to the original scattering problem: Find $w \in H^1(\Omega)$ such that

$$a(v, w) = (v, \xi) \quad \text{for all } v \in H^1(\Omega). \quad (20)$$

It can be verified that w is the weak solution to the following boundary value problem

$$\begin{cases} \Delta w + \kappa^2 w = -\xi & \text{in } \Omega, \\ \partial_\nu w = 0 & \text{on } \Gamma, \\ \partial_r w - \mathcal{T}^* w = 0 & \text{on } \partial B_R, \end{cases} \quad (21)$$

where the adjoint operator \mathcal{T}^* is defined as

$$(\mathcal{T}^* w)(R, \theta) = \frac{1}{R} \sum_{n \in \mathbb{Z}} \bar{h}_n(\kappa R) \hat{w}_n e^{in\theta}.$$

Following the same proof as that for the original scattering problem (9), we may show that the dual problem (20) has a unique weak solution, which satisfies the estimate

$$\|w\|_{H^1(\Omega)} \lesssim \|\xi\|_{L^2(\Omega)}. \quad (22)$$

The following lemma gives some energy representations of the error $\xi = u - u_h^N$ and is the basis for the a posteriori error analysis.

Lemma 1 *Let u, u_h^N , and w be the solutions to the problems (9), (17), and (20), respectively. We have*

$$\begin{aligned} \|\xi\|_{H^1(\Omega)}^2 &= \operatorname{Re}(a(\xi, \xi)) + \langle (\mathcal{T} - \mathcal{T}_N)\xi, \xi \rangle_{\partial B_R} \\ &\quad + \operatorname{Re}\langle \mathcal{T}_N \xi, \xi \rangle_{\partial B_R} + (\kappa^2 + 1)\|\xi\|_{L^2(\Omega)}^2, \end{aligned} \quad (23)$$

$$\|\xi\|_{L^2(\Omega)}^2 = a(\xi, w) + \langle (\mathcal{T} - \mathcal{T}_N)\xi, w \rangle_{\partial B_R} - \langle (\mathcal{T} - \mathcal{T}_N)\xi, w \rangle_{\partial B_R}, \quad (24)$$

$$\begin{aligned} a(\xi, \psi) + \langle (\mathcal{T} - \mathcal{T}_N)\xi, \psi \rangle &= \langle g, \psi - \psi_h \rangle_{\partial D} - a_N(u_h^N, \psi - \psi_h) \\ &\quad + \langle (\mathcal{T} - \mathcal{T}_N)u, \psi \rangle_{\partial B_R} \quad \text{for any } \psi \in H^1(\Omega), \psi_h \in V_h. \end{aligned} \quad (25)$$

Proof It follows from the definition of the sesquilinear form of a in (10) that

$$a(\xi, \xi) = (\nabla \xi, \nabla \xi) - \kappa^2 (\xi, \xi) - \langle \mathcal{T} \xi, \xi \rangle_{\partial B_R},$$

which gives

$$\|\xi\|_{H^1(\Omega)}^2 = a(\xi, \xi) + \langle \mathcal{T} \xi, \xi \rangle_{\partial B_R} + (\kappa^2 + 1)\|\xi\|_{L^2(\Omega)}^2.$$

Taking the real parts on both sides of the above equation yields (23). Taking $v = \xi$ in (20) gives (24). It remains to prove (25).

It follows from (9) and (17) that

$$\begin{aligned} a(\xi, \psi) &= a(u - u_h^N, \psi - \psi_h) + a(u - u_h, \psi_h) \\ &= \langle g, \psi - \psi_h \rangle_{\partial D} - a(u_h^N, \psi - \psi_h) + a(u - u_h^N, \psi_h) \\ &= \langle g, \psi - \psi_h \rangle_{\partial D} - a_N(u_h^N, \psi - \psi_h) \\ &\quad + \left(a_N(u_h^N, \psi - \psi_h) - a(u_h^N, \psi - \psi_h) \right) + \left(a(u, \psi_h) - a(u_h^N, \psi_h) \right). \end{aligned}$$

Noting that $a(u, \psi_h) = \langle g, \psi_h \rangle_{\partial D} = a_N(u_h^N, \psi_h)$, we have

$$\begin{aligned} a(\xi, \psi) &= \langle g, \psi - \psi_h \rangle_{\partial D} - a_N(u_h^N, \psi - \psi_h) + \left(a_N(u_h^N, \psi) - a(u_h^N, \psi) \right) \\ &= \langle g, \psi - \psi_h \rangle_{\partial D} - a_N(u_h^N, \psi - \psi_h) + \langle (\mathcal{T} - \mathcal{T}_N)u_h^N, \psi \rangle_{\partial B_R} \\ &= \langle g, \psi - \psi_h \rangle_{\partial D} - a_N(u_h^N, \psi - \psi_h) - \langle (\mathcal{T} - \mathcal{T}_N)\xi, \psi \rangle_{\partial B_R} \\ &\quad + \langle (\mathcal{T} - \mathcal{T}_N)u, \psi \rangle_{\partial B_R}, \end{aligned}$$

which implies (25).

It is necessary to estimate (25) and the last term in (24) in order to prove Theorem 1. We first show a trace regularity result.

Lemma 2 *For any $u \in H^1(\Omega)$, we have*

$$\|u\|_{H^{1/2}(\partial B_R)} \lesssim \|u\|_{H^1(\Omega)}, \quad \|u\|_{H^{1/2}(\partial B_{R'})} \lesssim \|u\|_{H^1(\Omega)}.$$

Proof Consider the annulus

$$B_R \setminus \bar{B}_{R'} = \{(r, \theta) : R' < r < R, 0 < \theta < 2\pi\}.$$

It is clear to note that $B_R \setminus \bar{B}_{R'} \subset \Omega$. A simple calculation yields

$$\begin{aligned} (R - R')|\zeta(R)|^2 &= \int_{R'}^R |\zeta(r)|^2 dr + \int_{R'}^R \int_r^R \frac{d}{dt} |\zeta(t)|^2 dt dr \\ &\leq \int_{R'}^R |\zeta(r)|^2 dr + (R - R') \int_{R'}^R 2|\zeta(r)||\zeta'(r)| dr, \end{aligned}$$

which implies by Young's inequality that

$$|\zeta(R)|^2 \leq (1 + (R - R')^{-1}) \int_{R'}^R (1 + n^2)^{1/2} |\zeta(r)|^2 dr + \int_{R'}^R (1 + n^2)^{-1/2} |\zeta'(r)|^2 dr.$$

Hence we have

$$\begin{aligned} (1 + n^2)^{1/2} |\zeta(R)|^2 &\leq (1 + (R - R')^{-1}) \int_{R'}^R (1 + n^2) |\zeta(r)|^2 dr + \int_{R'}^R |\zeta'(r)|^2 dr \\ &\leq (1 + (R - R')^{-1}) \int_{R'}^R ((1 + n^2) |\zeta(r)|^2 + |\zeta'(r)|^2) dr \end{aligned}$$

Given $u \in H^1(\Omega)$, it follows from the definitions of the $H^{1/2}(\partial B_R)$ norm (5) and the $H^1(\Omega)$ norm (4) that we have

$$\|u\|_{H^{1/2}(\partial B_R)}^2 = 2\pi \sum_{n \in \mathbb{Z}} (1 + n^2)^{1/2} |\hat{u}_n(R)|^2$$

and

$$\|u\|_{H^1(B_R \setminus B_{R'})}^2 = 2\pi \sum_{n \in \mathbb{Z}} \int_{R'}^R \left(\left(r + \frac{n^2}{r} \right) |\hat{u}_n(r)|^2 + r |\hat{u}'_n(r)|^2 \right) dr.$$

Combining the above estimates gives

$$\begin{aligned} \|u\|_{H^{1/2}(\partial B_R)}^2 &\leq 2\pi (1 + (R - R')^{-1}) \sum_{n \in \mathbb{Z}} \int_{R'}^R \left((1 + n^2) |\hat{u}_n(r)|^2 + |\hat{u}'_n(r)|^2 \right) dr \\ &\lesssim 2\pi \sum_{n \in \mathbb{Z}} \int_{R'}^R \left(\left(r + \frac{n^2}{r} \right) |\hat{u}_n(r)|^2 + r |\hat{u}'_n(r)|^2 \right) dr \\ &= \|u\|_{H^1(B_R \setminus B_{R'})}^2 \leq \|u\|_{H^1(\Omega)}^2. \end{aligned}$$

Similarly, the second estimate can be proved by observing that

$$(R - R') |\zeta(R')|^2 = \int_{R'}^R |\zeta(r)|^2 dr + \int_{R'}^R \int_r^{R'} \frac{d}{dt} |\zeta(t)|^2 dt dr,$$

which completes the proof.

Lemma 3 *Let u be the solution to (9). We have*

$$|\hat{u}_n(R)| \lesssim \left(\frac{R'}{R} \right)^{|n|} |\hat{u}_n(R')|.$$

Proof It is known that the solution of the scattering problem (1)–(3) admits the series expansion

$$u(r, \theta) = \sum_{n \in \mathbb{Z}} \frac{H_n^{(1)}(\kappa r)}{H_n^{(1)}(\kappa R')} \hat{u}_n(R') e^{in\theta}, \quad \hat{u}_n(R') = \frac{1}{2\pi} \int_0^{2\pi} u(R', \theta) e^{-in\theta} d\theta. \quad (26)$$

for all $r > R'$. Evaluating (26) at $r = R$ yields

$$u(R, \theta) = \sum_{n \in \mathbb{Z}} \frac{H_n^{(1)}(\kappa R)}{H_n^{(1)}(\kappa R')} \hat{u}_n(R') e^{in\theta},$$

which implies

$$\hat{u}_n(R) = \frac{H_n^{(1)}(\kappa R)}{H_n^{(1)}(\kappa R')} \hat{u}_n(R').$$

Using the asymptotic expression in (14), we obtain

$$|\hat{u}_n(R)| = \left| \frac{H_n^{(1)}(\kappa R)}{H_n^{(1)}(\kappa R')} \right| |\hat{u}_n(R')| \lesssim \left(\frac{R'}{R} \right)^{|n|} |\hat{u}_n(R')|,$$

which completes the proof.

Lemma 4 For any $\psi \in H^1(\Omega)$, we have

$$\begin{aligned} & |a(\xi, \psi) + \langle (\mathcal{T} - \mathcal{T}_N)\xi, \psi \rangle_{\partial B_R}| \\ & \lesssim \left(\left(\sum_{T \in \mathcal{M}_h} \eta_T^2 \right)^{1/2} + \left(\frac{R'}{R} \right)^N \|g\|_{L^2(\partial D)} \right) \|\psi\|_{H^1(\Omega)}. \end{aligned}$$

Proof Define

$$\begin{aligned} J_1 &= \langle g, \psi - \psi_h \rangle_{\partial D} - a_N(u_h^N, \psi - \psi_h), \\ J_2 &= \langle (\mathcal{T} - \mathcal{T}_N)u, \psi \rangle_{\partial B_R}, \end{aligned}$$

where $\psi_h \in V_h$. It follows from (25) that

$$a(\xi, \psi) + \langle (\mathcal{T} - \mathcal{T}_N)\xi, \psi \rangle_{\partial B_R} = J_1 + J_2.$$

By the definition of the sesquilinear form (18), J_1 can be rewritten as

$$\begin{aligned} J_1 &= \sum_{T \in \mathcal{M}_h} \left(\int_T (-\nabla u_h^N \cdot \nabla(\bar{\psi} - \bar{\psi}_h) + \kappa^2 u_h^N (\bar{\psi} - \bar{\psi}_h)) dx \right. \\ & \quad \left. + \sum_{e \in \partial T \cap \partial B_R} \int_e \mathcal{T}_N u_h^N (\bar{\psi} - \bar{\psi}_h) ds + \sum_{e \in \partial T \cap \Gamma} \int_e g(\bar{\psi} - \bar{\psi}_h) ds \right). \end{aligned}$$

Using the integration by parts, we get

$$\begin{aligned} J_1 &= \sum_{T \in \mathcal{M}_h} \left(\int_T (\Delta u_h^N + \kappa^2 u_h^N)(\bar{\psi} - \bar{\psi}_h) dx - \sum_{e \in \partial T} \int_e \nabla u_h^N \cdot \nu (\bar{\psi} - \bar{\psi}_h) ds \right. \\ & \quad \left. + \sum_{e \in \partial T \cap \partial B_R} \int_e \mathcal{T}_N u_h^N (\bar{\psi} - \bar{\psi}_h) ds + \sum_{e \in \partial T \cap \Gamma} \int_e g(\bar{\psi} - \bar{\psi}_h) ds \right) \\ &= \sum_{T \in \mathcal{M}_h} \left(\int_T \mathcal{R} u_h^N (\bar{\psi} - \bar{\psi}_h) dx + \sum_{e \in \partial T} \frac{1}{2} \int_e J_e (\bar{\psi} - \bar{\psi}_h) ds \right) \end{aligned}$$

Now we take $\psi_h = \Pi_h \psi \in V_h$. Here Π_h is the Scott–Zhang interpolation operator, which has the following interpolation estimates:

$$\|v - \Pi_h v\|_{L^2(T)} \lesssim h_T \|\nabla v\|_{L^2(\tilde{T})}, \quad \|v - \Pi_h v\|_{L^2(e)} \lesssim h_e^{1/2} \|\nabla v\|_{L^2(\tilde{e})}.$$

Here \tilde{T} and \tilde{e} are the union of all the elements in \mathcal{M}_h , which have nonempty intersection with the element T and the side e , respectively. It follows from the Cauchy–Schwarz inequality and the interpolation estimates that

$$\begin{aligned} |J_1| &\lesssim \sum_{T \in \mathcal{M}_h} \left(h_T \|\mathcal{R} u_h^N\|_{L^2(T)} \|\nabla \psi\|_{L^2(\tilde{T})} + \sum_{e \in \partial T} \frac{1}{2} h_e^{1/2} \|J_e\|_{L^2(e)} \|\nabla \psi\|_{L^2(\tilde{e})} \right) \\ &\lesssim \sum_{T \in \mathcal{M}_h} \left(h_T \|\mathcal{R} u_h^N\|_{L^2(T)} + \left(\sum_{e \in \partial T} \frac{1}{2} h_e \|J_e\|_{L^2(e)}^2 \right)^{1/2} \right) \|\psi\|_{H^1(\Omega)}, \end{aligned}$$

where the trace theorem is used. Using (19), we immediately get

$$|J_1| \lesssim \left(\sum_{T \in \mathcal{M}_h} \eta_T^2 \right)^{1/2} \|\psi\|_{H^1(\Omega)}.$$

It follows from the definitions of (7) and (16) that

$$\begin{aligned} |J_2| &= |\langle (\mathcal{T} - \mathcal{T}_N)u, \psi \rangle_{\partial B_R}| = \left| \frac{2\pi}{R} \sum_{|n| > N} h_n(\kappa R) \hat{u}_n(R) \bar{\hat{\psi}}_n(R) \right| \\ &\leq \left(\frac{2\pi}{R} \right) \sum_{|n| > N} |h_n(\kappa R)| |\hat{u}_n(R)| |\hat{\psi}_n(R)|. \end{aligned}$$

Using Lemma 3, we obtain

$$\begin{aligned} |J_2| &\lesssim \sum_{|n| > N} 2\pi |h_n(\kappa R)| \left(\frac{R'}{R} \right)^{|n|} |\hat{u}_n(R')| |\hat{\psi}_n(R)| \\ &\lesssim \left(\frac{R'}{R} \right)^N \sum_{|n| > N} 2\pi |h_n(\kappa R)| |\hat{u}_n(R')| |\hat{\psi}_n(R)|. \end{aligned}$$

It is shown in [14] that

$$|h_n(\kappa R)| \lesssim (1 + n^2)^{1/2} \lesssim |n|, \quad (27)$$

which together with Lemma 3 yields

$$\begin{aligned} |J_2| &\lesssim \left(\frac{R'}{R} \right)^N \left(\sum_{|n| > N} 2\pi (1 + n^2)^{1/2} |\hat{u}_n(R')|^2 \right)^{1/2} \left(\sum_{|n| > N} 2\pi (1 + n^2)^{1/2} |\hat{\psi}_n(R)|^2 \right)^{1/2} \\ &\lesssim \left(\frac{R'}{R} \right)^N \|u\|_{H^{1/2}(\partial B_{R'})} \|\psi\|_{H^{1/2}(\partial B_R)} \lesssim \left(\frac{R'}{R} \right)^N \|u\|_{H^1(\Omega)} \|\psi\|_{H^1(\Omega)}. \end{aligned}$$

Using the stability estimate (12), we get

$$|J_2| \lesssim \left(\frac{R'}{R} \right)^N \|g\|_{L^2(\partial D)} \|\psi\|_{H^1(\Omega)}.$$

Combining the above estimates yields

$$|J_1 + J_2| \lesssim \left(\left(\sum_{T \in \mathcal{M}_h} \eta_T^2 \right)^{1/2} + \left(\frac{R'}{R} \right)^N \|g\|_{L^2(\partial D)} \right) \|\psi\|_{H^1(\Omega)},$$

which completes the proof.

Lemma 5 *Let w be the solution of the dual problem (20). We have*

$$|\langle (\mathcal{T} - \mathcal{T}_N)\xi, w \rangle_{\partial B_R}| \lesssim N^{-2} \|\xi\|_{H^1(\Omega)}^2.$$

Proof It follows from (27), the Cauchy–Schwarz inequality, and Lemma 2 that

$$\begin{aligned}
| \langle (\mathcal{T} - \mathcal{T}_N)\xi, w \rangle_{\partial B_R} | &\leq 2\pi \sum_{|n|>N} |h_n(kR)| |\hat{\xi}_n(R)| |\hat{w}_n(R)| \lesssim 2\pi \sum_{|n|>N} |n| |\hat{\xi}_n(R)| |\hat{w}_n(R)| \\
&= 2\pi \sum_{|n|>N} \left((1+n^2)^{1/2} |n|^3 \right)^{-1/2} (1+n^2)^{1/4} |\hat{\xi}_n(R)| |n|^{5/2} |\hat{w}_n(R)| \\
&\lesssim \max_{|n|>N} \left((1+n^2)^{1/2} |n|^3 \right)^{-1/2} \left(2\pi \sum_{|n|>N} (1+n^2)^{1/2} |\hat{\xi}_n(R)|^2 \right)^{1/2} \\
&\quad \times \left(\sum_{|n|>N} |n|^5 |\hat{w}_n(R)|^2 \right)^{1/2} \\
&\lesssim N^{-2} \|\xi\|_{H^{1/2}(\partial B_R)} \left(\sum_{|n|>N} |n|^5 |\hat{w}_n(R)|^2 \right)^{1/2} \\
&\lesssim N^{-2} \|\xi\|_{H^1(\Omega)} \left(\sum_{|n|>N} |n|^5 |\hat{w}_n(R)|^2 \right)^{1/2}.
\end{aligned}$$

Next we consider the dual problem (21) in the annulus $B_R \setminus \bar{B}_{R'}$ in order to estimate $\hat{w}_n(R)$, i.e.,

$$\begin{cases} \Delta w + \kappa^2 w = -\xi & \text{in } B_R \setminus \bar{B}_{R'}, \\ w = w(R', \theta) & \text{on } \partial B_{R'}, \\ \partial_r w - \mathcal{T}^* w = 0 & \text{on } \partial B_R. \end{cases}$$

In the Fourier domain, we obtain a two-point boundary value problem for the coefficient \hat{w}_n :

$$\begin{cases} \frac{d^2 \hat{w}_n(r)}{dr^2} + \frac{1}{r} \frac{d\hat{w}_n(r)}{dr} + \left(\kappa^2 - \frac{n^2}{r^2} \right) \hat{w}_n(r) = -\hat{\xi}_n(r), & R' < r < R, \\ \frac{d\hat{w}_n(R)}{dr} - \frac{1}{R} \bar{h}_n(\kappa R) \hat{w}_n(R) = 0, & r = R, \\ \hat{w}_n(R') = \hat{w}_n(R'), & r = R'. \end{cases}$$

It follows from the variation of parameters that the solution of the above second order equation is

$$\begin{aligned}
\hat{w}_n(r) &= S_n(r) \hat{w}_n(R') + \frac{i\pi}{4} \int_{R'}^r t W_n(r, t) \hat{\xi}_n(t) dt \\
&\quad + \frac{i\pi}{4} \int_{R'}^R t S_n(t) W_n(R', r) \hat{\xi}_n(t) dt, \tag{28}
\end{aligned}$$

where

$$S_n(r) = \frac{H_n^{(2)}(\kappa r)}{H_n^{(2)}(\kappa R')}, \quad W_n(r, t) = \det \begin{bmatrix} H_n^{(1)}(\kappa r) & H_n^{(2)}(\kappa r) \\ H_n^{(1)}(\kappa t) & H_n^{(2)}(\kappa t) \end{bmatrix}.$$

Taking $r = R$ in (28), we get

$$\hat{w}_n(R) = S_n(R)\hat{w}_n(R') + \frac{i\pi}{4} \int_{R'}^R t S_n(R) W_n(R', t) \hat{\xi}_n(t) dt,$$

which yields

$$|\hat{w}_n(R)| \leq |S_n(R)| |\hat{w}_n(R')| + \frac{\pi}{4} \int_{R'}^R t |S_n(R)| |W_n(R', t)| |\hat{\xi}_n(t)| dt.$$

We may easily get from the asymptotic expressions (13) and (14) that

$$S_n(R) \sim \left(\frac{R'}{R}\right)^{|n|} \quad \text{as } n \rightarrow \infty$$

and

$$\begin{aligned} W_n(R', t) &= 2i J_n(\kappa R') Y_n(\kappa R') \left(\frac{J_n(\kappa t)}{J_n(\kappa R')} - \frac{Y_n(\kappa t)}{Y_n(\kappa R')} \right) \\ &\sim -\frac{2i}{\pi |n|} \left(\left(\frac{t}{R'}\right)^{|n|} - \left(\frac{R'}{t}\right)^{|n|} \right) \quad \text{as } n \rightarrow \infty. \end{aligned}$$

Thus, we obtain

$$|S_n(R)| \lesssim \left(\frac{R'}{R}\right)^{|n|} \quad \text{and} \quad |W_n(R', t)| \lesssim |n|^{-1} \left(\frac{t}{R'}\right)^{|n|}.$$

Combining the above estimates yields

$$\begin{aligned} |\hat{w}_n(R)| &\lesssim \left(\frac{R'}{R}\right)^{|n|} |\hat{w}_n(R')| + |n|^{-1} \left(\frac{R'}{R}\right)^{|n|} \|\hat{\xi}_n(t)\|_{L^\infty([R', R])} \int_{R'}^R t \left(\frac{t}{R'}\right)^{|n|} dt \\ &\lesssim \left(\frac{R'}{R}\right)^{|n|} |\hat{w}_n(R')| + n^{-2} \|\hat{\xi}_n(t)\|_{L^\infty([R', R])}. \end{aligned} \quad (29)$$

For any $t \in [R', R]$, without loss of generality, we assume that t is closer to the left endpoint R' than the right endpoint R . Denote $\delta = R - R'$. Then we have $R - t \geq \delta/2$. Thus

$$\begin{aligned} |\hat{\xi}_n(t)|^2 &= \frac{1}{R-t} \int_R^t \left((R-s) |\hat{\xi}_n(s)|^2 \right)' ds \\ &= \frac{1}{R-t} \int_R^t \left(-|\hat{\xi}_n(s)|^2 + 2(R-s) \operatorname{Re}(\hat{\xi}'_n(s) \bar{\hat{\xi}}_n(s)) \right) ds \\ &\leq \frac{1}{R-t} \int_t^R |\hat{\xi}_n(s)|^2 ds + 2 \int_{R'}^R |\hat{\xi}_n(s)| |\hat{\xi}'_n(s)| ds, \end{aligned}$$

which implies that

$$\begin{aligned} \|\hat{\xi}_n(t)\|_{L^\infty([R', R])}^2 &\leq \frac{2}{\delta} \|\hat{\xi}_n(t)\|_{L^2([R', R])}^2 + 2 \|\hat{\xi}_n(t)\|_{L^2([R', R])} \|\hat{\xi}'_n(t)\|_{L^2([R', R])} \\ &\leq \left(\frac{2}{\delta} + |n| \right) \|\hat{\xi}_n(t)\|_{L^2([R', R])}^2 + |n|^{-1} \|\hat{\xi}'_n(t)\|_{L^2([R', R])}^2. \end{aligned} \quad (30)$$

Using (29) and (30) gives

$$\begin{aligned} \sum_{|n|>N} |n|^5 |\hat{w}_n(R)|^2 &\lesssim \sum_{|n|>N} |n|^5 \left(\left(\frac{R'}{R} \right)^{|n|} |\hat{w}_n(R')| + n^{-2} \|\hat{\xi}_n(t)\|_{L^\infty([R',R])} \right)^2 \\ &\lesssim \sum_{|n|>N} |n|^5 \left(\left(\frac{R'}{R} \right)^{2|n|} |\hat{w}_n(R')|^2 + n^{-4} \|\hat{\xi}_n(t)\|_{L^\infty([R',R])}^2 \right) \\ &= I_1 + I_2, \end{aligned}$$

where

$$I_1 = \sum_{|n|>N} |n|^5 \left(\frac{R'}{R} \right)^{2|n|} |\hat{w}_n(R')|^2 \quad \text{and} \quad I_2 = \sum_{|n|>N} |n| \|\hat{\xi}_n(t)\|_{L^\infty([R',R])}^2.$$

Noting that the function $t^4 e^{-t}$ is bounded on $(0, +\infty)$, we have

$$I_1 \lesssim \max_{|n|>N} \left(|n|^4 \left(\frac{R'}{R} \right)^{2|n|} \right) \sum_{|n|>N} |n| |\hat{w}_n(R')|^2 \lesssim \|w\|_{H^{1/2}(\partial B_{R'})}^2 \lesssim \|\xi\|_{H^1(\Omega)}^2$$

and

$$\begin{aligned} I_2 &\lesssim \sum_{|n|>N} \left(|n| \left(\frac{2}{\delta} + |n| \right) \|\hat{\xi}_n\|_{L^2([R',R])}^2 + \|\hat{\xi}'_n\|_{L^2([R',R])}^2 \right) \\ &\leq \sum_{|n|>N} \left(\left(\frac{2}{\delta} |n| + n^2 \right) \|\hat{\xi}(t)\|_{L^2([R',R])}^2 + \|\hat{\xi}'(t)\|_{L^2([R',R])}^2 \right). \end{aligned} \quad (31)$$

A simple calculation yields

$$\begin{aligned} \|\xi\|_{H^1(B_R \setminus B_{R'})}^2 &= 2\pi \sum_{n \in \mathbb{Z}} \int_{R'}^R \left(\left(r + \frac{n^2}{r} \right) |\hat{\xi}_n(r)|^2 + r |\hat{\xi}'_n(r)|^2 \right) dr \\ &\geq 2\pi \sum_{n \in \mathbb{Z}} \int_{R'}^R \left(\left(R' + \frac{n^2}{R} \right) |\hat{\xi}_n(r)|^2 + R' |\hat{\xi}'_n(r)|^2 \right) dr. \end{aligned} \quad (32)$$

It is easy to note that

$$\frac{2}{\delta} |n| + n^2 \lesssim R' + \frac{n^2}{R}. \quad (33)$$

It follows from (31)–(33) that

$$I_2 \lesssim \|\xi\|_{H^1(B_R \setminus B_{R'})}^2 + \frac{1}{R'} \|\xi\|_{H^1(B_R \setminus B_{R'})}^2 \lesssim \|\xi\|_{H^1(B_R \setminus B_{R'})}^2 \leq \|\xi\|_{H^1(\Omega)}^2.$$

Therefore, we have

$$\sum_{|n|>N} |n|^5 |\hat{w}_n(R)|^2 \lesssim \|\xi\|_{H^1(\Omega)}^2,$$

which completes the proof.

We now prove the main conclusion.

Proof It is easy to verify from (16) and (27) that

$$\operatorname{Re}\langle \mathcal{T}_N \xi, \xi \rangle_{\partial B_R} = 2\pi \sum_{|n| \leq N} \operatorname{Re}(h_n(\kappa R)) |\hat{\xi}_n|^2 \leq 0.$$

It follows from (23) and Lemma 4 that there exist two positive constants C_1 and C_2 independent of h and N such that

$$\|\xi\|_{H^1(\Omega)}^2 \leq C_1 \left(\left(\sum_{T \in \mathcal{M}_h} \eta_T^2 \right)^{1/2} + \left(\frac{R'}{R} \right)^N \|g\|_{L^2(\partial D)} \right) \|\xi\|_{H^1(\Omega)} + C_2 \|\xi\|_{L^2(\Omega)}^2.$$

Using (24), Lemma 4, (22), and Lemma 5, we obtain

$$\|\xi\|_{L^2(\Omega)}^2 \leq C_3 \left(\left(\sum_{T \in \mathcal{M}_h} \eta_T^2 \right)^{1/2} + \left(\frac{R'}{R} \right)^N \|g\|_{L^2(\partial D)} \right) \|\xi\|_{L^2(\Omega)} + C_4 N^{-2} \|\xi\|_{H^1(\Omega)}^2,$$

where $C_3 > 0$ and $C_4 > 0$ are independent of h and N . Combining the above two estimates, we have

$$\begin{aligned} \|\xi\|_{H^1(\Omega)}^2 &\leq (C_1 + C_2 C_3) \left(\left(\sum_{T \in \mathcal{M}_h} \eta_T^2 \right)^{1/2} + \left(\frac{R'}{R} \right)^N \|g\|_{L^2(\partial D)} \right) \|\xi\|_{H^1(\Omega)} \\ &\quad + C_2 C_4 N^{-2} \|\xi\|_{H^1(\Omega)}^2. \end{aligned}$$

Choose a sufficiently large integer N_0 such that $C_2 C_4 N_0^{-2} \leq 1/2$, which completes the proof by taking $N > N_0$.

5 Implementation and numerical examples

In this section, we discuss the implementation of the adaptive finite element algorithm with the truncated DtN boundary condition and present two numerical examples to demonstrate the competitive performance of the proposed method.

5.1 Adaptive algorithm

Based on the a posteriori error estimate from Theorem 1, we use the PDE toolbox of MATLAB to implement the adaptive algorithm of the linear finite element formulation. It is shown in Theorem 1 that the a posteriori error estimate consists of two parts: the finite element discretization error ϵ_h and the truncation error ϵ_N which depends on N , where

$$\epsilon_h = \left(\sum_{T \in \mathcal{M}_h} \eta_T^2 \right)^{1/2} = \eta_{\mathcal{M}_h}, \quad (34)$$

$$\epsilon_N = \left(\frac{R'}{R} \right)^N \|g\|_{L^2(\partial D)}. \quad (35)$$

1	Given the tolerance $\epsilon > 0, \theta \in (0, 1)$;
2	Fix the computational domain $\Omega = B_R \setminus \bar{D}$ by choosing the radius R ;
3	Choose R' and N such that $\epsilon_N \leq 10^{-8}$;
4	Construct an initial triangulation \mathcal{M}_h over Ω and compute error estimators;
5	While $\epsilon_h > \epsilon$ do
6	choose $\hat{\mathcal{M}}_h \subset \mathcal{M}_h$ according to the strategy $\eta_{\hat{\mathcal{M}}_h} > \theta \eta_{\mathcal{M}_h}$;
7	refine all the elements in $\hat{\mathcal{M}}_h$ and obtain a new mesh denoted still by \mathcal{M}_h ;
8	solve the discrete problem (17) on the new mesh \mathcal{M}_h ;
9	compute the corresponding error estimators;
10	End while.

Table 1 The adaptive DtN-FEM algorithm.

In the implementation, we can choose R' , R , and N based on (35) such that the finite element discretization error is not contaminated by the truncation error, or more specifically, ϵ_N is required to be very small compared with ϵ_h , say, $\epsilon_N \leq 10^{-8}$. For simplicity, in the following numerical experiments, R' is chosen such that the scatterer lies exactly in the circle $B_{R'}$, and N is taken to be the smallest positive integer satisfying $\epsilon_N \leq 10^{-8}$. Table 1 shows the adaptive finite element algorithm with the DtN boundary condition for solving the scattering problem (9).

5.2 Numerical experiments

We report two numerical examples to demonstrate the effectiveness of the proposed method. In particular, we compare the method with the adaptive finite element method with the perfectly matched layer (PML) [9]. In our implementation, we set the wave number by $\kappa = 2\pi$, which accounts for the wavelength $\lambda = 2\pi/\kappa = 1$, and take $\theta = 0.5$ in Table 1. For comparison, the complex coordinate stretching of the PML method is defined by

$$\tilde{x} = x(1 + i\sigma(r - R)) \quad \text{for all } x \in \mathbb{R}^2 \setminus \bar{B}_R,$$

where $r = |x|$ and $\sigma > 0$ is a positive constant and is taken as $\sigma = 5$.

Example 1. Let the obstacle $D = B_1$ be the unit ball and $\Omega = B_2$. In (2), the boundary condition g is chosen such that the exact solution is

$$u(x) = H_0^{(1)}(\kappa|x|). \quad (36)$$

We set $R' = 1$ in the algorithm. For the adaptive PML method, the thickness of the PML is set by $\rho = 2$ so that the error of PML approximation is negligible.

Table 2 compares the numerical results by using adaptive mesh refinement and the uniform mesh refinement. Clearly, it shows the advantage of using adaptive mesh refinements. Moreover, it is shown that the a posteriori error estimate ϵ_h provides a rather good estimate for the priori error $e_h = \|\nabla(u - u_h^N)\|_{L^2(\Omega)}$. Figure 2 displays the curves of $\log e_h$ and $\log \epsilon_h$ versus $\log \text{DoF}_h$ for our adaptive DtN method and the adaptive PML method, where DoF_h denotes the number of nodal points of the mesh \mathcal{M}_h in the domain Ω for our DtN method or in the domain which is composed of Ω and the PML layer for the PML method. It indicates that for both of the two methods, the meshes and the associated numerical complexity are quasi-optimal, i.e., $\|\nabla(u - u_h^N)\|_{L^2(\Omega)} = \mathcal{O}(\text{DoF}_h^{-1/2})$ holds asymptotically.

Table 2 Comparison of numerical results using adaptive mesh and uniform mesh refinements for Example 1. DoF_h is the number of nodal points of mesh \mathcal{M}_h .

Adaptive mesh				Uniform mesh			
DoF_h	e_h	ϵ_h	ϵ_h/e_h	DoF_h	e_h	ϵ_h	ϵ_h/e_h
132	0.5358	0.5712	1.0661	132	0.5358	0.5712	1.0661
529	0.3393	0.3645	1.0743	478	0.3592	0.3860	1.0745
1490	0.1911	0.2232	1.1646	1812	0.1698	0.2086	1.2280
6563	0.0870	0.1117	1.1680	7048	0.0826	0.1071	1.2975
17721	0.0428	0.0549	1.2827	27792	0.0414	0.0544	1.3163

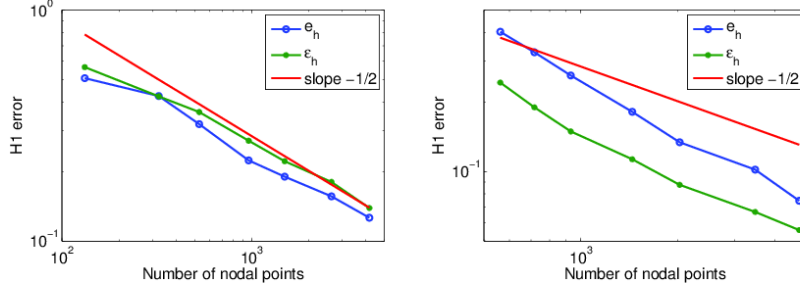


Fig. 2 Quasi-optimality of the a priori and a posteriori error estimates for Example 1. (left) the adaptive DtN method; (right) the adaptive PML method.

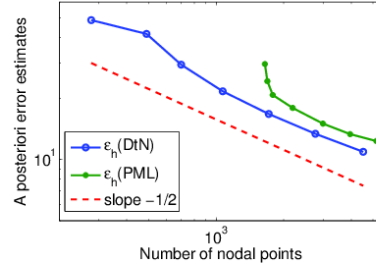


Fig. 3 Quasi-optimality of the a posteriori error estimates for Example 2.

Example 2. This example concerns the scattering of the plane wave $u^{\text{inc}} = e^{i\kappa x_1}$ by a U-shaped obstacle D which is contained in the box $\{(x_1, x_2) : -2.0 < x_1 < 2.2, -0.7 < x_2 < 0.7\}$. There is no analytical solution for this example and the solution contains singularity around the corners of the obstacle. The Neumann boundary condition is set by $g = \partial_\nu u^{\text{inc}}$ on ∂D . We take $R = 3, R' = 2.31$ for the adaptive DtN method and set the thickness of the PML by $\rho = 3$ for the adaptive PML method.

Figure 3 shows the curve of $\log \epsilon_h$ versus $\log \text{DoF}_h$. It implies that the decay of the a posteriori error estimates are $\mathcal{O}(\text{DoF}_h^{-1/2})$ for both of the two algorithms. The adaptive meshes are plotted in Figure 4 for the two methods. The adaptive DtN method generates locally refined meshes of Ω , while the adaptive PML method produces automatically coarse mesh size away from the outer boundary of Ω . Figure 5 shows the surface plot of the amplitudes of the associated numerical solutions restricted in Ω .

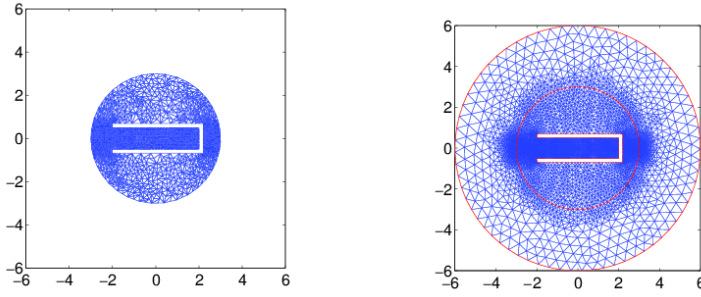


Fig. 4 An adaptively refined mesh (left) with 3037 elements using the adaptive DtN method and (right) with 6644 elements using the adaptive PML method for Example 2.

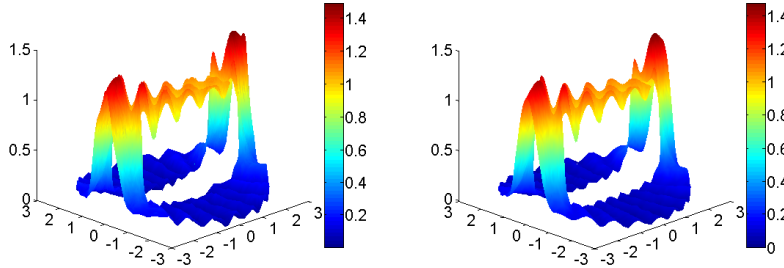


Fig. 5 The surface plot of the amplitude of the associated numerical solution restricted in Ω on the mesh of Figure 4 for Example 2. (left) the adaptive DtN method; (right) the adaptive PML method.

Based on the above observation, we conclude that the adaptive DtN method is comparable in accuracy, efficiency, and robustness to the adaptive PML method.

6 Conclusion

Based on the a posteriori error estimate, we presented an adaptive finite element method with DtN boundary condition for the acoustic obstacle scattering problem. Numerical results show that the proposed method is competitive with the adaptive PML method. This work provides a viable alternative to the adaptive finite element method with PML for solving the same problem and enriches the range of choices available for solving many other wave propagation problems. We hope that the method can be applied to other scientific areas where the problems are proposed in unbounded domains, especially in the areas where the PML technique might not be applicable. Future work is to extend our analysis to the adaptive DtN finite element method for solving the three-dimensional electromagnetic obstacle scattering problem, where the wave propagation is governed by Maxwell's equations.

Acknowledgements The research of X.J. was supported in part by China NSF grant 11401040 and by the Fundamental Research Funds for the Central Universities 24820152015RC17. The

research of P.L. was supported in part by the NSF grant DMS-1151308. The research of J.L. was partially supported by the China NSF grants 11126040 and 11301214. The author of W.Z. was supported in part by China NSF 91430215, by the Funds for Creative Research Groups of China (grant 11321061), and by the National Magnetic Confinement Fusion Science Program (2015GB110003).

References

1. Babuška, I., Aziz, A.: Survey Lectures on Mathematical Foundations of the Finite Element Method. in *The Mathematical Foundations of the Finite Element Method with Application to the Partial Differential Equations*. ed. by A. Aziz, Academic Press, New York, 5–359 (1973).
2. Bayliss, A., Turkel, E.: Radiation boundary conditions for numerical simulation of waves. *Comm. Pure Appl. Math.* **33**, 707–725 (1980).
3. Bao, G.: Finite element approximation of time harmonic waves in periodic structures. *SIAM J. Numer. Anal.* **32**, 1155–1169 (1995).
4. Bao, G., Chen, Z., Wu, H.: Adaptive finite element method for diffraction gratings. *J. Opt. Soc. Amer. A* **22**, 1106–1114 (2005).
5. Bao, G., Li, P., Wu, H.: An adaptive edge element method with perfectly matched absorbing layers for wave scattering by periodic structures. *Math. Comp.* **79**, 1–34 (2010).
6. Bao, G., Wu, H.: Convergence analysis of the perfectly matched layer problems for time-harmonic Maxwells equations. *SIAM J. Numer. Anal.* **43**, 2121–2143 (2005).
7. Berenger, J.-P.: A perfectly matched layer for the absorption of electromagnetic waves. *J. Comput. Phys.* **114**, 185–200 (1994).
8. Chen, Z., Wu, H.: An adaptive finite element method with perfectly matched absorbing layers for the wave scattering by periodic structures. *SIAM J. Numer. Anal.* **41**, 799–826 (2003).
9. Chen, Z., Liu, X.: An adaptive perfectly matched layer technique for time-harmonic scattering problems. *SIAM J. Numer. Anal.* **43**, 645–671 (2005).
10. Collino, F., Monk, P.: The perfectly matched layer in curvilinear coordinates. *SIAM J. Sci. Comput.* **19**, 2061–2090 (1998).
11. Colton, D., Kress, R.: *Integral Equation Methods in Scattering Theory*. John Wiley & Sons, New York (1983).
12. Colton, D., Kress, R.: *Inverse Acoustic and Electromagnetic Scattering Theory*. Second Edition, Springer, Berlin, New York (1998).
13. Engquist, B., Majda, A.: Absorbing boundary conditions for the numerical simulation of waves. *Math. Comp.* **31**, 629–651 (1977).
14. O. G. Ernst, A finite-element capacitance matrix method for exterior Helmholtz problems, *Numer. Math.* **75** (1996) 175–204.
15. Grote, M., Keller, J.: On nonreflecting boundary conditions. *J. Comput. Phys.* **122**, 231–243 (1995).
16. Grote, M., Kirsch, C.: Dirichlet-to-Neumann boundary conditions for multiple scattering problems. *J. Comput. Phys.* **201**, 630–650 (2004).
17. Hagstrom, T.: Radiation boundary conditions for the numerical simulation of waves. *Acta Numerica*, 47–106 (1999).
18. Hsiao, G.C., Nigam, N., Pasciak, J.E., Xu, L.: Error analysis of the DtN-FEM for the scattering problem in acoustics via Fourier analysis. *J. Comput. Appl. Math.* **235**, 4949–4965 (2011).
19. Jiang, X., Li, P., Zheng, W.: Numerical solution of acoustic scattering by an adaptive DtN finite element method. *Commun. Comput. Phys.* **13**, 1227–1244 (2013).
20. Jin, J.: *The Finite Element Method in Electromagnetics*. New York: Wiley (1993).
21. Monk, P.: *Finite Element Methods for Maxwell’s Equations*. Clarendon Press, Oxford (2003).
22. Schatz, A.H.: An observation concerning Ritz–Galerkin methods with indefinite bilinear forms. *Math. Comp.* **28**, 959–962 (1974).
23. Teixeira, F.L., Chew, W.C.: Advances in the theory of perfectly matched layers. in *Fast and Efficient Algorithms in Computational Electromagnetics*, W. C. Chew et al., eds., Artech House, Boston, 283–346 (2001).

-
24. Turkel, E., Yefet, A.: Absorbing PML boundary layers for wave-like equations. *Appl. Numer. Math.* **27**, 533–557 (1998).
 25. Wang, Z., Bao, G., Li, J., Li, P., Wu, H.: An adaptive finite element method for the diffraction grating problem with transparent boundary condition. *SIAM J. Numer. Anal.* **53**, 1585–1607 (2015).
 26. Watson, G.N.: *A Treatise on the Theory of Bessel Functions*. Cambridge University Press, Cambridge, UK (1922).